A Self-Consistent Static Model of the Double-Heterostructure Laser

DANIEL P. WILT AND AMNON YARIV, FELLOW, IEEE

Abstract—A new static model of the double-heterostructure laser is presented which treats the p-n junction in the laser in a consistent manner. The solution makes use of the finite-element method to treat complex diode geometries. The model is valid above lasing threshold and shows both the saturation in the diode junction voltage at threshold as well as lateral mode shifts associated with spatial hole burning. Several geometries have been analyzed and some specific results are presented as illustration.

I. Introduction

DOUBLE-HETEROSTRUCTURE injection lasers have recently become objects of intense interest as compact, highly efficient sources of coherent light. With this in mind, laser diode modeling is potentially a tool of great value, both to understand the effects seen in real laser diodes as well as to predict and possibly optimize the behavior of as yet unfabricated devices.

A large number of authors have constructed highly simplified and idealized models of the double-heterostructure injection laser to illustrate qualitatively the effects of material and structural parameters on device behavior [1]. These models are quite useful to correlate observed laser current thresholds with device parameters, but are of little use in understanding the device behavior above threshold. This, however, is one of the most important aspects of laser diode performance.

There are at present several general models of the laser diode above lasing threshold [2]-[6]. However, these models make assumptions about the electrical characteristics of the diode that are incorrect. Specifically, in each model the diode p-n junction is assumed to behave according to

$$j = j_0 \exp \frac{q\varphi}{nkT} \tag{1}$$

where j represents the injected electron and hole current densities (which are assumed to be equal), j_0 and n are material parameters, q is the electronic charge, φ is the junction voltage, k is Boltzmann's constant, and T is the absolute temperature. This is not a fundamental relationship. It can be derived for a one-dimensional p-n junction from more fundamental relationships. The use of this relationship in laser diode modeling, even as an approximation, neglects two very important effects: first, the effect on the electrical characteristics of lateral carrier drift and diffusion and, second, the saturation of junction voltage (and carrier populations) associated with lasing threshold. A more reasonable condition to apply to the diode junction in the double-heterostructure laser is to assume the continuity of the carrier quasi-Fermi levels across the heterojunction interfaces. This assumption leads naturally to the saturation of the diode voltage at lasing threshold, and is consistent with semiconductor physics. However, the use of this model of the diode junction requires the use of a different solution method from that of previous models.

Another model specifically designed to treat the behavior of a narrow planar stripe laser treats the diode junction in this manner using a highly simplified geometry [7]. The simplifications involved in this model, however, make it impossible to generalize.

In this paper, a model of the double-heterostructure laser diode is presented which treats the diode junction in the manner described above. Fundamental relationships that describe the device electrical and optical characteristics are derived and simultaneously solved in a self-consistent manner to yield both the electrical and optical behavior of the device. The model is designed for use both above and below lasing threshold. To give as much freedom as possible in the treatment of device geometry, the finite-element method is adopted as a solution technique. A number of interesting geometries have been examined and some specific results will be presented.

To begin with, some simplifying assumptions will be made. It should be stressed that these are not fundamental limitations of the model, but rather good approximations that can be applied to a large fraction of the device geometries in use.

First, since longitudinal effects are minor in most devices, only a lateral, two-dimensional model will be used. All longitudinal variations will be averaged over. Second, the active layer in the device will be assumed to be thin compared to the carrier diffusion lengths, so that electron and hole densities can be assumed to be constant across the active layer thickness. Third, cladding layer bandgaps will be assumed to be large enough so that minority carrier leakage from the active layer can be neglected compared to the majority carrier densities. This leads to the simplification that outside the active layer we need only solve an ohmic conduction problem. Fourth, the diode waveguide is assumed to be treatable by the effective permittivity method.

We now break up the model into two coupled subproblems, the electrical model and the optical model.

Manuscript received January 27, 1981; revised April 20, 1981. This work was supported by the Office of Naval Research and the National Science Foundation under the Optical Communication Program.

D. P. Wilt was with the California Institute of Technology, Pasadena, CA 91125. He is now with Bell Laboratories, Murray Hill, NJ 07974.

A. Yariv is with the California Institute of Technology, Pasadena, CA 91125.

0018-9197/81/0900-1941$00.75

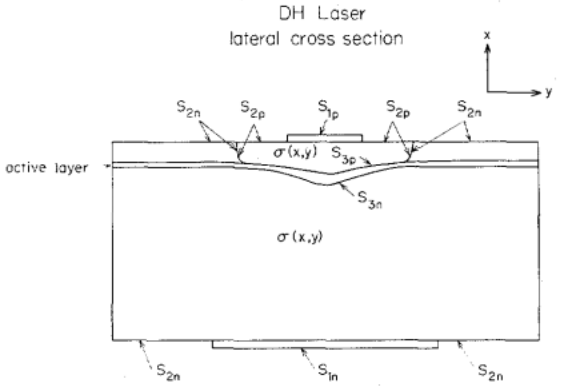

Fig. 1. Lateral cross section of the typical double-heterostructure laser.

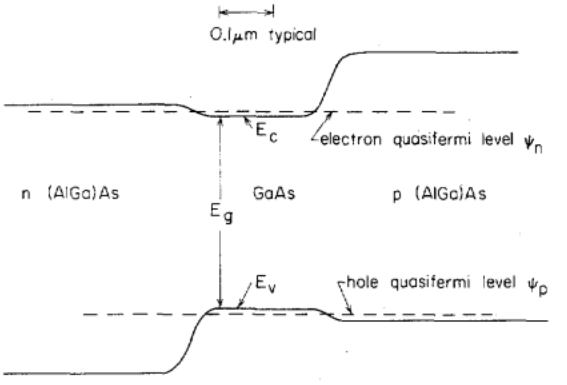

Fig. 2. Representative band structure diagram for the diode junction in a double-heterostructure laser under high forward bias.

II. The Electrical Model

The typical geometry of the device modeled is presented in Fig. 1. It consists of two ohmic conduction regions, one a p-type semiconductor, the other an n-type semiconductor, and a thin active layer that is partially surrounded by isotype cladding, in this case n-type, and partially sandwiched in between p-type and n-type cladding. The only cases excluded at this time are those where injection occurs from a remote junction or across a homojunction in the active layer. As stated, the problem with regard to the electrical characteristics of the device breaks into four coupled problems: two ohmic conduction problems in the isotype cladding layers, and two continuity relationships in the active layer.

In the two isotype cladding layers we solve Laplace's equation:

$$\nabla \cdot (\sigma \nabla \varphi_p) = 0 \tag{2}$$

$$\nabla \cdot (\sigma \nabla \varphi_n) = 0 \tag{3}$$

where σ is the conductivity and φ_p and φ_n are the electrostatic potentials in either region. These equations are subject to the boundary conditions $\varphi_p = \varphi_{p0}$ on S_{1p} and $\varphi_n = \varphi_{n0}$ on S_{1n}, the equipotential ohmic contacts of the device; $\sigma \vec{n} \cdot \nabla \varphi_p = 0$ on S_{2p} and $\sigma \vec{n} \cdot \nabla \varphi_n = 0$ on S_{2n}, the open surfaces where no normal current flows; and $\varphi_p = \varphi_p(y)$ on S_{3p} and $\varphi_n = \varphi_n(y)$ on S_{3n}, the heterojunction interfaces where the potential will be assumed to be a function of the lateral coordinate to the interface. The outward pointing normal to the surfaces is represented by $\vec{n}$.

The solution to this problem yields the injected current densities into the active layer:

$$j_{p,inj} = -\sigma \vec{n} \cdot \nabla \varphi_p \text{ on } S_{3p} \tag{4}$$

$$j_{n,inj} = -\sigma \vec{n} \cdot \nabla \varphi_n \text{ on } S_{3n} \tag{5}$$

and the electrostatic potential inside each of the regions, which for self-consistency must be related to the potential distribution along the active layer.

This relationship is provided in the model presented here by the boundary condition on the heterojunction interfaces and the semiconductor continuity relations. This is in contrast to [2]-[6] where (1) is used for this purpose. In comparison, the resulting relationship used here between injected current and junction voltage is both implicit and nonlocal, making the solution much more difficult.

Referring to Fig. 2, we have drawn a representative band diagram of the p-n heterojunction interface under forward bias. The detailed spike structure at the interfaces is assumed to be washed out by interfacial mixing, as occurs in liquid phase epitaxial material. In this diagram, the carrier quasi-Fermi levels appear as straight lines due to the assumption that the active layer is thin compared to the diffusion length. In the case of the active layer surrounded by isotype cladding, again the continuity of the quasi-Fermi levels is assumed.

With this assumption and Poisson's equation for the electrostatic potential in the active layer

$$\nabla^2 \varphi = \frac{\rho}{\epsilon \epsilon_0} \tag{6}$$

where φ is the electrostatic potential, ρ is the charge density, ϵ is the relative permittivity, and ϵ_0 is the permittivity of free space; we can relate the electron and hole densities in the active layer to the potential difference across the p-n heterojunction. Noting that the typical Debye length for these devices is on the order of 100 Å, we will assume quasi-neutrality and write

$$p + N_d^+ = n + N_a^- \tag{7}$$

$$p = \frac{2}{\sqrt{\pi}} N_v F_{1/2}\left(\frac{E_v - \psi_p}{kT}\right) \tag{8}$$

$$n = \frac{2}{\sqrt{\pi}} N_c F_{1/2}\left(\frac{\psi_n - E_c}{kT}\right) \tag{9}$$

$$E_c - E_v = E_g \tag{10}$$

$$\psi_n - \psi_p = e(\varphi_p - \varphi_n). \tag{11}$$

n and p are the electron and hole densities, N_d^+ and N_a^- are the ionized donor and acceptor densities, N_c and N_v are the effective densities of states in the conduction and valence bands, ψ_n and ψ_p are electron and hole quasi-Fermi levels, E_c and E_v are conduction and valence band edges, E_g is the bandgap of the active layer, and φ_n and φ_p are the electrostatic potentials on either side of the p-n heterojunction. $F_{1/2}$ is the Fermi function:

$$F_{1/2}(\eta_f) = \int_0^\infty \frac{\sqrt{\eta}\, d\eta}{e^{\eta - \eta_f} + 1}. \tag{12}$$

These equations completely define the electron and hole densities as a function of the potential difference across the p-n heterojunction.

To relate the injected current density now to the potential along the active layer, we must look at the continuity relationships:

$$\frac{dp}{dt} = G_p - U_p - \frac{1}{e}\nabla \cdot \vec{J}_p = 0 \tag{13}$$

$$\frac{dn}{dt} = G_n - U_n + \frac{1}{e}\nabla \cdot \vec{J}_n = 0. \tag{14}$$

G_n and G_p are electron and hole generation rates, U_n and U_p are electron and hole recombination rates, and $\vec{J}_n$ and $\vec{J}_p$ are electron and hole drift and diffusion currents.

Injected current can most easily be included in these equations as a generation term. Thermal generation is neglectable in the laser diode, which operates under high forward bias:

$$G_p = \frac{j_{p,inj}}{et} \tag{15}$$

$$G_n = -\frac{j_{n,inj}}{et} \tag{16}$$

where t is the active layer thickness.

The recombination terms consist of both nonradiative (trap, surface recombination) and radiative (spontaneous and stimulated) terms. The forms used for these are

$$U_{p,\text{trap}} = U_{n,\text{trap}} = \frac{pn}{p\tau_n + n\tau_p} \tag{17}$$

$$U_{p,\text{surface}} = U_{n,\text{surface}} = \frac{S\delta(y - y_s)pn}{p + n} \tag{18}$$

$$U_{p,\text{spont}} = U_{n,\text{spont}} = Bpn \tag{19}$$

$$U_{p,\text{stim}} = U_{n,\text{stim}} = \frac{Pg}{\hbar\omega}. \tag{20}$$

τ_n and τ_p are effective nonradiative minority carrier lifetimes and may include the effects of leakage over the confining heterojunction barriers. S is a surface recombination velocity, y_s being the location of the surface interface. B is a material constant, P is the optical power density, g is the local optical gain of the medium, and $\hbar\omega$ is the photon energy. In this model, the gain term is assumed to be of the form

$$g = g_0 + g_{1p}p + g_{1n}n + g_{2pn}pn. \tag{21}$$

These relationships are simplified forms of more general relationships, making use of the fact that the laser diode operates in the high forward bias regime. Of course, to be consistent with the assumption that the active layer is thin and that the electron and hole densities are uniform across it, the relationship for the stimulated emission recombination rate (20) must be averaged over the direction normal to the active layer.

The drift and diffusion term that appears in these equations requires more elaboration. Using the degenerate Einstein relations, we have

$$\vec{J}_p = p\mu_p \nabla \psi_p \tag{22}$$

$$\vec{J}_n = n\mu_n \nabla \psi_n \tag{23}$$

where μ_n and μ_p are the electron and hole mobilities. An additional and important complication that we wish to include is the case where the active layer thickness may vary. Since we have already separated off the injected current densities from drift and diffusion currents, we must be careful to force the drift and diffusion current to flow parallel to the heterojunction interfaces, or equivalently, to conserve carriers. We can assume that the magnitude of the current flow is constant across the active layer, but the changing of the active layer thickness gives an additional term when we take the divergence in (13) and (14). With the condition that active layer thickness varies slowly with respect to y, we have for these terms

$$-\frac{1}{e}\nabla \cdot \vec{J}_p = -\frac{1}{e}\left(\frac{1}{t}\cdot\frac{dt}{dy} + \frac{d}{dy}\right)\left(p\mu_p \frac{d\psi_p}{dy}\right) \tag{24}$$

$$\frac{1}{e}\nabla \cdot \vec{J}_n = \frac{1}{e}\left(\frac{1}{t}\cdot\frac{dt}{dy} + \frac{d}{dy}\right)\left(n\mu_n \frac{d\psi_n}{dy}\right). \tag{25}$$

These terms are easily seen to be conservative, as desired. The derivatives of the quasi-Fermi levels that appear in these terms must, of course, be treated self-consistently with the solution to the ohmic conduction problem. The identification is provided by the assumption of continuity of quasi-Fermi levels across the interfaces, as before. Neglecting the contribution of carriers that leak over the confining heterobarriers, this allows us to identify ψ_p with the Fermi level in the p-cladding and ψ_n with the Fermi level in the n-cladding along the p-n junction region. In the case where the active layer is surrounded by isotype cladding, we do this for the majority carrier; for the minority carrier we instead demand that the injected minority carrier current density be zero.

With these relationships, the electrical behavior of the device is completely defined. It is interesting to note that at no point in the analysis was the assumption of equal injected current densities or the assumption of ambipolar diffusion required. These are not necessarily bad approximations, but they cannot be derived from the relationships above. The difficulty lies in the fact that the electron and hole populations are essentially in equilibrium with their isotype cladding layers. An interesting facet of this is that symmetric devices with p- and n-type layers interchanged but with identical conductivities do not behave identically.

From the standpoint of solving the electrical behavior of the model, the problem is to find an electrostatic potential distribution and quasi-Fermi levels in the active layer that are consistent with all of the relationships set down above.

III. The Optical Model

The optical model presented here is quite similar to that presented elsewhere [2]-[6]. In brief, effective permittivity formalism is used to find the TE modes of a perturbed slab waveguide. TE modes are treated because they are experi-

mentally known to dominate the behavior of the semiconductor laser. Modal gains are either found directly from the solution of the waveguide eigenmode equation or from perturbation theory if the mode profile is only slightly perturbed. Here double-heterostructure lasers split into two equivalence classes, those where carriers contribute significantly to the waveguide problem and those where carriers may be treated as a perturbation. Roughly speaking, these two classes correspond to devices with geometric structures that define the waveguide modes (e.g., buried heterostructure lasers [8] and channeled substrate lasers [9], [10]) and devices that have no built-in geometric waveguide structure (e.g., beryllium implanted lasers [11] and oxide-stripe lasers [12]). This is a rough division because there are important laser structures that have geometric waveguiding and still use the carrier populations to define the optical modes [13]. The optical model presented here, while for convenience limited to TE modes and effective index formalism, is capable of treating both classes of semiconductor lasers.

With the assumption of a TE mode, the eigen equation for the waveguide modes of the laser simplifies to

$$\left(\frac{\partial^2}{\partial x^2}+\frac{\partial^2}{\partial y^2}+k^2\epsilon(x,y)-\beta^2\right)u(x,y)=0 \tag{26}$$

where u is the (scalar) TE electric field and β is the mode propagation constant. The magnitude of the wave vector is k and ϵ represents the complex relative permittivity of the medium. For convenience, we will take the x coordinate to be normal to the active layer and the y coordinate parallel to the active layer. This eigen equation can be presented in variational form as

$$\delta\beta^2=\delta\left(\frac{\int_{-\infty}^{\infty}\int_{-\infty}^{\infty}dx\,dy\left(-\left(\frac{\partial u}{\partial x}\right)^2-\left(\frac{\partial u}{\partial y}\right)^2+k^2\epsilon u^2\right)}{\int_{-\infty}^{\infty}\int_{-\infty}^{\infty}dx\,dy\,u^2}\right)=0. \tag{27}$$

To apply the effective permittivity formalism to this equation, a variational form will be assumed and the variational principle (27) will be used to derive an Euler equation for the lateral modal field.

The procedure applied to the problem is to first solve the one-dimensional waveguide problem for the lowest mode X:

$$\left(\frac{\partial^2}{\partial x^2}+k^2\epsilon(x,y)-\gamma_1^2(y)\right)X(x,y)=0 \tag{28}$$

(an effective variation in the normal (x) direction to the active layer). The lateral coordinate y is considered here to be a parameter. Consistent with the use of complex permittivities, the normalization condition on this field will be taken as

$$\int_{-\infty}^{\infty}dx\,X^2=1. \tag{29}$$

We would now like to find then the best possible approximation to the true modal field using this field X to represent the variation in the perpendicular (x) direction. To do this, we substitute into the variational equation the trial form

$$u(x,y)=X(x,y)\,Y(y). \tag{30}$$

Since the function we will allow to vary, Y, is a function only of the lateral variable y, we can integrate out the variable x in the variational principle to get an effective variational principle involving only Y and y:

$$\delta\left(\frac{\int_{-\infty}^{\infty}dy\left(-\left(\frac{dY}{dy}\right)^2+(\gamma_1^2+\gamma_2^2)\,Y^2\right)}{\int_{-\infty}^{\infty}dy\,Y^2}\right)=0 \tag{31}$$

where

$$\gamma_2^2=\int_{-\infty}^{\infty}dx\left(-\left(\frac{\partial X}{\partial y}\right)^2\right). \tag{32}$$

The normalization condition (29) and the field equation for X, (28), have been used to simplify this expression.

The Euler equation for this variational expression is then

$$\left(\frac{d^2}{dy^2}+k^2\epsilon_{\text{eff}}-\beta^2\right)Y=0 \tag{33}$$

where the effective permittivity is

$$k^2\epsilon_{\text{eff}}=\gamma_1^2+\gamma_2^2. \tag{34}$$

The second term in this expression, γ_2^2, is usually quite small and is neglected here. This leaves us with the expression

$$k^2\epsilon_{\text{eff}}=\gamma_1^2 \tag{35}$$

for the effective permittivity. The field Y will be assumed normalized according to

$$\int_{-\infty}^{\infty}dy\,Y^2=1 \tag{36}$$

so that the normalization on the field u is

$$\int_{-\infty}^{\infty}\int_{-\infty}^{\infty}dx\,dy\,u^2=1. \tag{37}$$

The advantage of approaching the effective permittivity problem from the standpoint of the variational principle, aside from the inclusion of a term which we have neglected, is that it assures in a sense that the best approximation to the true modal field is found. If first-order perturbation theory is applied to the modal profiles found (assuming the extra term is not neglected), the lowest nonzero corrections to the modal field involve overlap integrals of the field X with higher order modes in the x direction, or equivalently, corrections involving overlap integrals of X with itself are not present.

The modal gain is related to the propagation constant β

$$g_{\text{mode}}=2\,\text{Im}\,\beta_{\text{mode}} \tag{38}$$

which, if the proper permittivity is used, is exact. If one wishes

to use a modal profile and propagation constant determined with a different permittivity, lowest order perturbation theory to find the propagation constant (and thus modal gain) is appropriate:

$$d(\beta^2) = \int_{-\infty}^{\infty} \int_{-\infty}^{\infty} dx\, dy\, u^2 k^2\, d\epsilon \tag{39}$$

which simplifies to

$$d\beta = \frac{k^2}{2\beta} \int_{-\infty}^{\infty} \int_{-\infty}^{\infty} dx\, dy\, u^2\, d\epsilon. \tag{40}$$

To treat a laser, one must, of course, include the effects of the longitudinal cavity. In the simplest form, these are the roundtrip phase condition (which is here neglected) to give the Fabry-Perot modes (often called longitudinal modes) and the roundtrip gain condition that the optical gain in the cavity balances the optical loss in the cavity plus the radiation losses. This model neglects the contribution of spontaneous emission to the optical power flow in the cavity, but, if desired, this contribution is easily included. This relationship can be stated as

$$g_{\text{mode}} = \alpha_{\text{mode}} + \frac{1}{L} \ln\left(\frac{1}{R_{\text{mode}}}\right) \tag{41}$$

where g_{mode} is the modal gain, α_{mode} is the modal loss, L is the device length, and R_{mode} is the mode mirror reflectivity.

The optical power density in the device can be represented as

$$P(x, y) = P_t \frac{|u(x, y)|^2}{\int_{-\infty}^{\infty} \int_{-\infty}^{\infty} dx\, dy\, |u(x, y)|^2} \tag{42}$$

where P_t is the total power flowing in the cavity (average over length of backward and forward traveling waves). This optical power is related to the actual power emitted from both mirrors by

$$P_0 = P_t \ln\left(\frac{1}{R}\right) \tag{43}$$

where P_0 is the total power output from the device. This can be shown in the following manner. The actual power distribution in the laser diode is

$$P(x, y, z) = P(x, y)\,(Z_+(z) + Z_-(z)). \tag{44}$$

The functions $Z_\pm(z)$ are given by

$$Z_\pm(z) = \frac{\sqrt{R} \ln\left(\frac{1}{R}\right)}{2(1 - R)} \exp \pm \frac{z}{L} \ln\left(\frac{1}{R}\right) \tag{45}$$

where the diode mirrors are located at $\pm L/2$. It is easily verified that the average over the length of the diode of (44) yields (42). The total power emitted from the laser facets is given by

$$P_0 = P_t(1 - R) \left(Z_+\left(\frac{L}{2}\right) + Z_-\left(-\frac{L}{2}\right)\right). \tag{46}$$

Evaluation of this expression yields (43).

In this model, the distributed loss term is assumed to be a constant, although its dependence upon p and n can easily be included in a manner similar to the gain expression (21).

Note, however, that this distributed loss is not equivalent to a gain term. The difference between the two is that the gain term also appears in the stimulated recombination rate [see (20)] while the loss term does not. This loss term represents nonretrievable loss mechanisms such as scattering.

This model assumes all optical modes to have the same facet reflectivity. This is probably a good approximation as we have taken them all to have the same mode profile X. The variation in facet reflectivity between modes can, of course, be included in the calculation with minor complication.

Depending upon which equivalence class the device under consideration is judged to fall into, geometrically guided or carrier guided, the lateral mode profiles can be found once and only perturbation theory can be applied to find the modal gain and loss, or the lateral mode profiles found for every value of the carrier populations, while the solution to the electrical problem is being iteratively sought. If the device is carrier guided, of course, the dependence of both real and imaginary parts of the permittivity on electron and hole density must be included in the modal calculation. In principle and practice, either type of device can be treated. However, for the carrier guided device, the solution of the eigenmode equation at each iteration can be quite time consuming. Hybrid techniques involving both exact and perturbation methods are usually more reasonable for this type of device.

IV. Solution Technique

As a first step, the functional relationship between the junction voltage and carrier population densities is solved [see (7)-(11)]. This is done using a nonlinear root-finding technique. Since this is only material dependent, it need be done only once for a given material and doping density.

The two ohmic conduction problems [(2)-(5)] are treated using the finite-element method with triangular elements and linear interpolation functions. Since this problem is linear, the solution can be stated in the form of an equivalent Green's function for each region that relates the injected current density to the potential distribution along the junction boundary:

$$\int dy\, j_{p,inj} f_i = \sum_j K^p_{i,j}(\varphi_{p0} - \varphi_{pj}) \tag{47}$$

$$\int dy\, j_{n,inj} f_i = \sum_j K^n_{i,j}(\varphi_{n0} - \varphi_{nj}) \tag{48}$$

where the potentials on the contacts are φ_{p0} and φ_{n0}, as before, and φ_{pj} and φ_{nj} are the nodal potentials along the junction interface. The potential along the junction interface is assumed to vary linearly between the junction nodes. The f_i are linear interpolation functions along the interface.

The problem then reduces to satisfying the continuity relationships in the active layer [see (13) and (14)] subject to (47) and (48). Simultaneously, of course, the optical modes of the structure and their stimulated emission (if they are

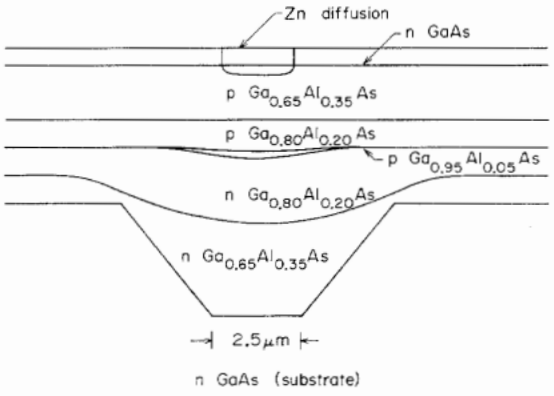

Fig. 3. Lateral cross section of the example device treated. This type of device is characterized as a nonplanar large optical cavity laser.

above threshold) must be included. If a mode is receiving stimulated emission, its gain is held constant according to (41). This problem, in order to be consistent with the solution of the ohmic conduction problem, is formulated also in the finite-element fashion. The electrical model here is one-dimensional and linear interpolation functions are used. The finite-element equations are derived using Galerkin's method. The optical mode problem is treated as both a slab waveguide problem [(28) for the mode profile X] and a finite-element problem [(33) for the mode profile Y] where a one-dimensional grid and first-order Hermite interpolation functions are used. Again this is done to achieve compatibility between the subproblems. Up to four lateral modes are included in the calculation.

In this formulation, the problem reduces to solving a nonlinear system of equations for the nodal values of the two quasi-Fermi levels ψ_p and ψ_n and the optical power outputs in each of the modes. The only free parameter in the model then is the voltage difference between the equipotential contacts, a global boundary condition. In practice this is allowed to vary and, instead, the total current through the device is specified. An iterative technique of the modified Newton form is used to find the appropriate solution to the nonlinear simultaneous equations.

V. Results

Several device structures have been analyzed, including both cases where carriers are treated as a perturbation and where carriers define the lateral optical mode structure. Lasers of the first type analyzed include the embedded laser [14] and the channeled substrate laser [9], [10]. Only one laser structure of the second type has been analyzed, the beryllium implanted laser [11]. Specific results are presented here for the laser structure of Burnham [10], which as been analyzed in simplified form by Streifer [6], [15]. Unfortunately, that analysis neglects the effect mentioned in connection with (24) and (25) and as a result the solution to the diffusion equation presented there is incorrect, as it does not conserve carriers.

The structure of the device is shown in Fig. 3. The material and structural parameters assumed for the device are listed in Tables I and II, respectively. The material parameters used are

TABLE I
Material Parameters Used in the Model

Parameter	Value
N_C	$4.7 \times 10^{17} \frac{1}{cm^3}$
N_V	$7 \times 10^{18} \frac{1}{cm^3}$
$N_a^- - N_d^+$	$3 \times 10^{17} \frac{1}{cm^3}$
τ_n, τ_p	1×10^{-7} sec
B	0.9×10^{-10} cm^3/s
μ_n	$4000 \frac{cm^2}{Vs}$
μ_p	$300 \frac{cm^2}{Vs}$
g_0	-180 cm^{-1}
g_{1p} g_{1n}	0
g_{2pn}	7×10^{-35} cm^5
α	12 cm^{-1}
$E_g, \hbar\omega$	1.43 eV
ℓ	2.5×10^{-2} cm
R	0.32

TABLE II
Structural Parameters for the Device Analyzed

layer	conductivity ohm^{-1} cm^{-1}	refractive index ($\epsilon = n^2$)
n^+ GaAs substrate	1000	3.64 -0.0528 i
n $Ga_{0.65}Al_{0.35}As$	200	3.39
n $Ga_{0.80}Al_{0.20}As$	200	3.50
p $Ga_{0.95}Al_{0.05}As$	-	3.64 + $dn_{carriers}$
p $Ga_{0.80}Al_{0.20}As$	8	3.50
p $Ga_{0.65}Al_{0.35}As$	8	3.39
n GaAs isolation	-	3.64 - 0.0528i

chosen to be compatible with both direct experimental measurements and measured broad-area lasing current threshold densities [1]. The n-GaAs top layer in the structure is used only as a blocking layer, which is shorted by the zinc diffused stripe, so the electrical model omits the top n-layer and considers the zinc diffusion as a 2 μm wide stripe contact. Refractive indexes are given instead of relative permittivities, where $\epsilon = n^2$. The substrate and contact layer may be omitted from the waveguide problem with the result that the effective permittivity is real.

The solution of the equations for electron and hole densities as a function of voltage difference across the heterojunction is shown in Fig. 4. Note that since the Fermi functions appropriate to degenerate semiconductors are used, the curves begin to bend over at high injection levels.

This device has an obvious mirror symmetry, and this will be exploited to ease the calculation. However, it must be remembered that with this simplification all currents and output powers should be doubled.

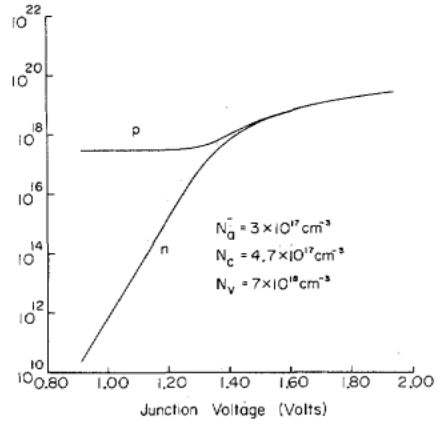

Fig. 4. The electron and hole densities in the active layer as a function of the voltage across the heterojunction.

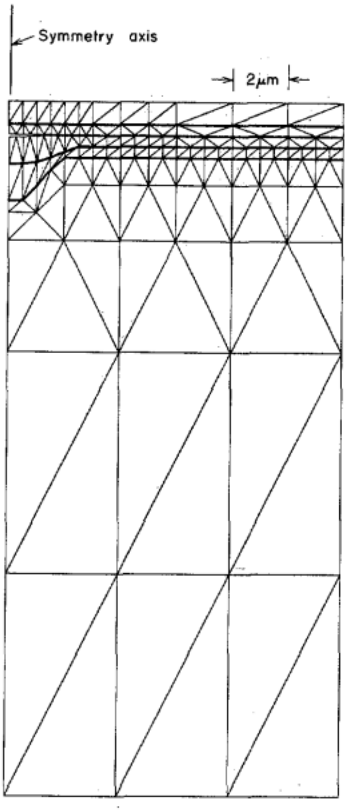

Fig. 5. The finite-element model constructed for the ohmic conduction problems. Use has been made of the device symmetry.

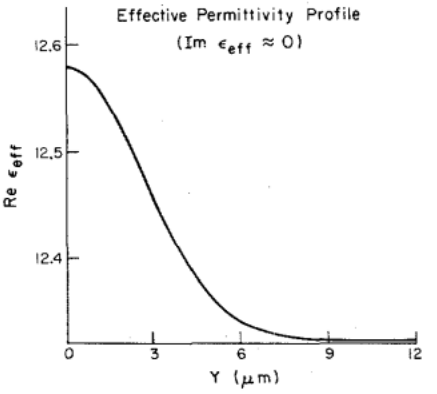

Fig. 6. The effective permittivity profile for the device. Use has been made of the device symmetry.

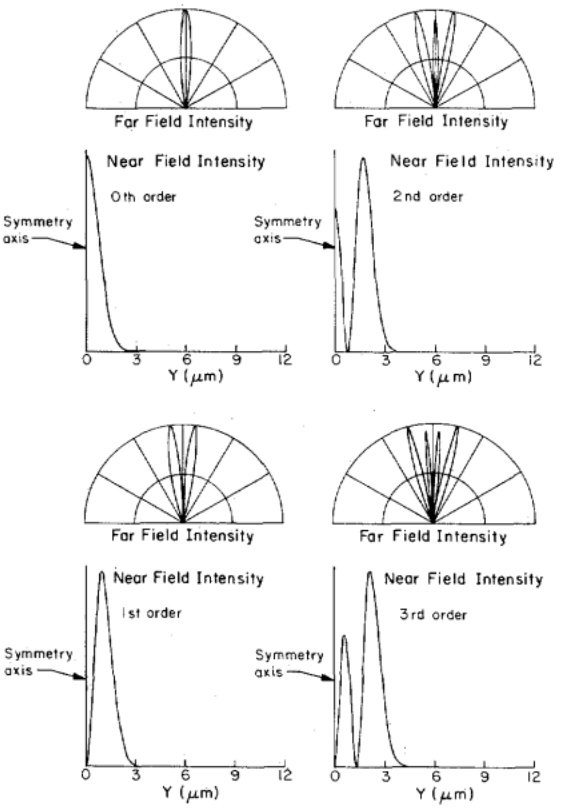

Fig. 7. The four lowest lateral modes (Y) of the device and their corresponding far-field patterns. Use has been made of the device symmetry.

The finite-element model used for the calculation of the Green's functions (47) and (48) is shown in Fig. 5. The use of a large number of elements for the modeling of the substrate is not necessary but does give the device a reasonable series resistance. In most situations, assuming the substrate-epilayer interface to be equipotential is a good approximation.

The geometric model of the device (see Fig. 3) is used for the calculation of the effective permittivity (35), and the lowest four lateral optical modes (Y) of the device are calculated as described. The active layer thickness is assumed to vary as

$$t = 0.08 + 0.2 \exp - 0.0732\, y^2 \qquad (49)$$

where t is the active layer thickness and y is the lateral distance measured from the center of the stripe, both measured in μm. The effective permittivity profile for the device is shown in Fig. 6 and the lowest four lateral modes and their corresponding far-field patterns are shown in Fig. 7. Since the waveguiding properties of this device are geometrically determined, (40) is used to determine modal gains for the device.

The solutions for the static device behavior with pump current as a parameter are shown in Figs. 8–11. Fig. 8 shows the current versus voltage characteristics of the device and clearly shows the saturation of the diode junction voltage at lasing threshold, which can be seen to occur at approximately

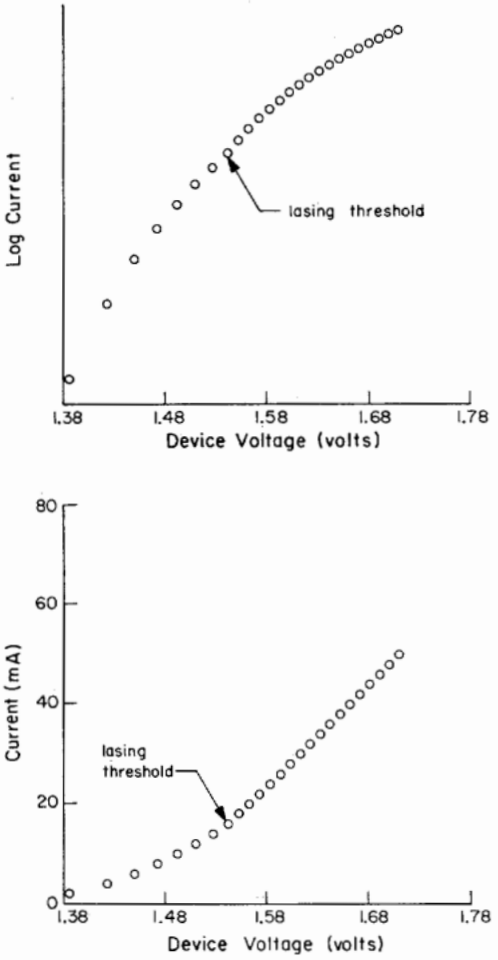

Fig. 8. The current–voltage characteristics of the device. To obtain total device current, the scale should be doubled.

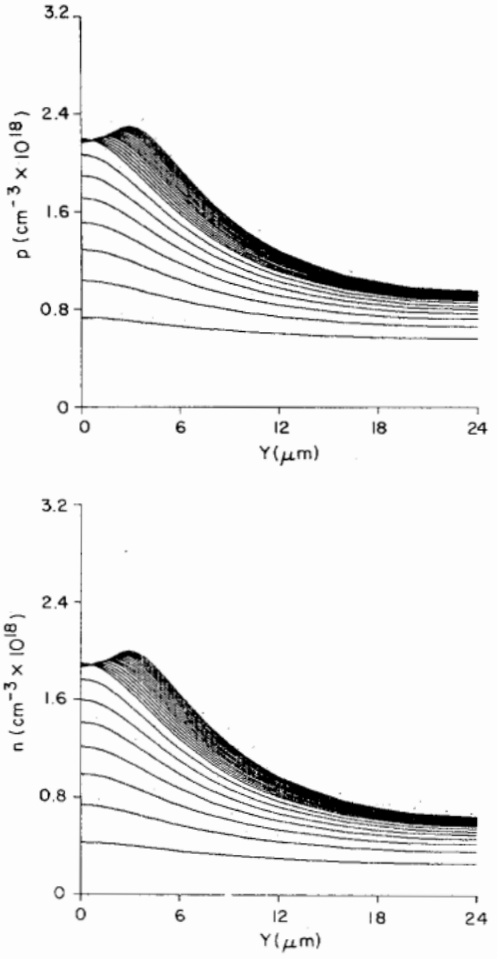

Fig. 9. The lateral carrier density profiles for the device in operation. Total device current is varied as a parameter from 4 to 100 mA with a step of 4 mA.

31 mA of total device current. Above threshold, further increases in device voltage are due to the finite device resistance, here approximately 2.4 Ω. The carrier profiles for the device with the pump current as a parameter are shown in Fig. 9. The saturation of the carrier populations at lasing threshold and the effects of spatial hole burning can be seen. This is a different effect from the "diffusion focusing" described in [15]. The light versus current characteristics of the device are shown in Fig. 10, where stimulated power output to each mode as well as modal gains are plotted as functions of pump current. The total power output as a function of pump current is shown in Fig. 11. The effect of spatial hole burning can be seen to eventually let higher order modes of the structure emit stimulated power. The kink associated with the first-order mode beginning to lase at approximately 52 mA total current and 20 mW total power output is clearly visible. These results are in agreement with the experimental results for this device.

To compare with the results presented in [6] and [15], the sheet resistance for the p-layers assumed here is approximately 500 Ω. The calculated threshold current in [15] for this sheet resistance and a 2 μm wide stripe contact is 53.7 mA. In this model, the injected carrier profile at threshold falls to half of its value at the center of the stripe at a lateral distance of 10 μm. In comparison, [15] yields 6 μm for this distance. In addition, the above threshold analysis in [6], although for a different structure, shows a different type of spatial hole burning than this model. In that calculation, spatial hole burning was found to significantly lower the carrier population at the center of the stripe under lasing conditions. In this model, the carrier population at the center of the stripe is nearly constant above threshold and lateral mode switching results from the increase in the carrier population outside the lasing mode. This difference can be attributed directly to the p-n junction boundary conditions applied in the two models.

VI. Summary and Conclusions

In summary, a model of the double-heterostructure laser has been presented that correctly treats the diode junction of the device. It is valid above threshold and is capable of treating a large number of the device geometries in use. With this model, the quantitative behavior of devices can be investigated above lasing threshold and compared and optimized.

References

[1] For some examples and more references, see Chapter 7 of H. C. Casey, Jr. and M. B. Panish, *Heterostructure Lasers: Part B, Materials and Operating Characteristics.* New York: Academic, 1978.

[2] J. Buus, "A model for the static properties of DH lasers," *IEEE J. Quantum Electron.*, vol. QE-15, pp. 734–749, Aug. 1979.

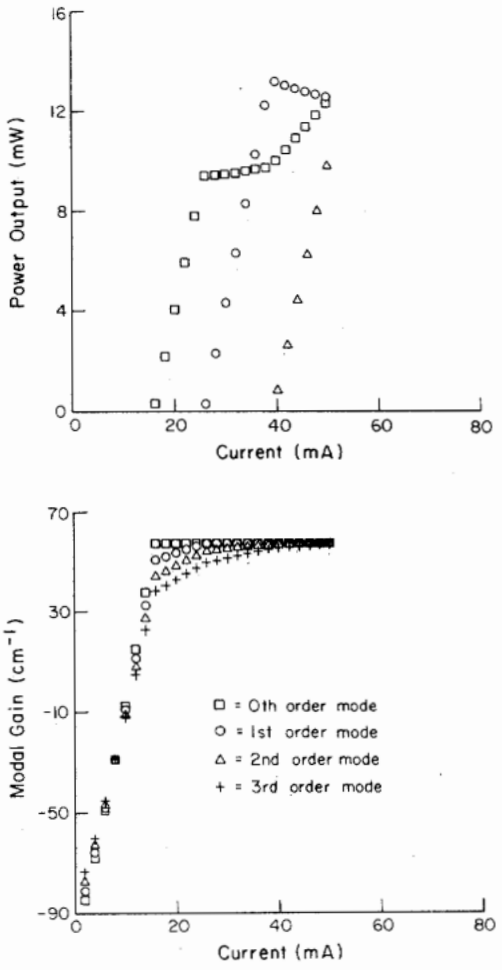

Fig. 10. The light versus current characteristics and modal gains for the device. Each lateral mode is plotted separately. To obtain total device current and power, the scales should be doubled.

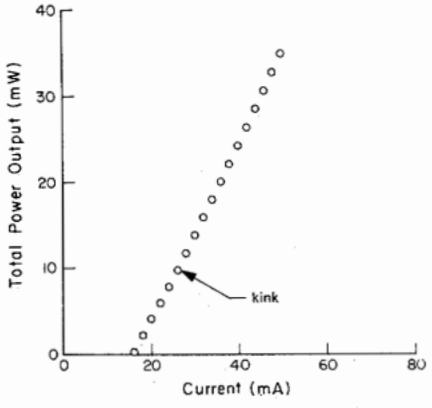

Fig. 11. The light versus current characteristics for the device, with output powers in the lateral modes summed. To obtain total device current and power, the scales should be doubled.

[3] K. A. Shore, T. E. Rozzi, and G. H. in't Veld, "Semiconductor laser analysis: General method for characterising devices of various cross sectional geometries," *IEE Proc.*, pt. I, vol. 127, pp. 221–229, 1980.
[4] N. Chinone, "Nonlinearity in power-output-current characteristics of stripe-geometry injection lasers," *J. Appl. Phys.*, vol. 48, pp. 3237–3243, 1977.
[5] R. Lang, "Lateral transverse mode instability and its stabilization in stripe geometry injection lasers," *IEEE J. Quantum Electron.*, vol. QE-15, pp. 718–726, Aug. 1979.
[6] W. Streifer, D. R. Scifres, and R. D. Burnham, "Above threshold analysis of double heterostructure lasers with laterally tapered active regions," *Appl. Phys. Lett.*, vol. 37, pp. 877–879, 1980.
[7] P. M. Asbeck, D. A. Cammack, J. J. Daniele, and V. Klebanoff, "Lateral mode behavior in narrow stripe lasers," *IEEE J. Quantum Electron.*, vol. QE-15, pp. 727–733, Aug. 1979.
[8] T. Tsukada, "GaAs-$Ga_xAl_{1-x}As$ buried heterostructure injection lasers," *J. Appl. Phys.*, vol. 45, pp. 4899–4906, 1974.
[9] K. Aiki, M. Nakamura, T. Kuroda, and J. Umeda, "Channelled-substrate planar structure (AlGa)As injection lasers," *Appl. Phys. Lett.*, vol. 30, pp. 649–651, 1977.
[10] R. D. Burnham, D. R. Scifres, W. Streifer, and S. Peled, "Nonplanar large optical cavity GaAs/GaAlAs semiconductor laser," *Appl. Phys. Lett.*, vol. 35, pp. 734–736, 1979.
[11] N. Bar-Chaim, M. Lanir, S. Margalit, I. Ury, D. Wilt, M. Yust, and A. Yariv, "Be implanted (GaAl)As stripe geometry lasers," *Appl. Phys. Lett.*, vol. 36, pp. 233–235, 1980.
[12] Y. Yonezu, I. Sakuma, K. Kobayashi, T. Kamejima, M. Ueno, and Y. Nannichi, "A GaAs-$Al_xGa_{1-x}As$ double heterostructure planar stripe laser," *Japan. J. Appl. Phys.*, vol. 12, pp. 1585–1592, 1973.
[13] D. Botez, "CW high-power single-mode lasers using constricted double heterostructures with a large optical cavity (CDH-LOC)," *Top. Meet. Integrated Guided Wave Optics*, Incline Village, NV, Jan. 1980, paper MC2.
[14] J. Katz, S. Margalit, D. Wilt, P. C. Chen, and A. Yariv, "Single growth embedded epitaxy AlGaAs injection lasers with extremely low threshold currents," *Appl. Phys. Lett.*, vol. 37, pp. 987–989, 1980.
[15] W. Streifer, R. D. Burnham, and D. R. Scifres, "Analysis of diode lasers with lateral spatial variations in thickness," *Appl. Phys. Lett.*, vol. 37, pp. 121–123, 1980.

Daniel P. Wilt was born in Elyria, OH, on August 30, 1954. He received the B.A. degree in mathematics and physics from the University of Southern California, University Park, in 1976 and the Ph.D. degree in applied physics from the California Institute of Technology, Pasadena, in June 1981.

In July of 1981 he joined the staff at Bell Laboratories, Murray Hill, NJ, where he is currently pursuing research in the field of semiconductor lasers.

Dr. Wilt is a member of Phi Beta Kappa and Phi Kappa Phi.

Amnon Yariv (S'56–M'59–F'70), for a photograph and biography, see p. 1394 of the August 1981 issue of this JOURNAL.